Reactions of tetrakis(trifluoromethyl)diphosphine and bis(trifluoromethyl)phosphine with ruthenium carbonyl clusters; X-ray structure of tetraruthenium carbonyl cluster derivatives

H.G. Ang [a,*], S.G. Ang [a], S.W. Du [a], B.H. Sow [a], A.L. Rheingold [b]

[a] *Department of Chemistry, National University of Singapore, Lower Kent Ridge Road, Singapore 0511, Singapore*
[b] *Department of Chemistry and Center for Catalytic Science and Technology, University of Delaware, Newark, DE 19716, USA*

Abstract

Reaction of $[Ru_3(CO)_{12}]$ with $(CF_3)_2P-P(CF_3)_2$ in p-xylene at 140°C yielded the compounds $[Ru_4(CO)_{13}\{\mu-P(CF_3)_2\}_2]$ (1), $[Ru_4(CO)_{14}\{\mu-P(CF_3)_2\}_2]$ (2) and $[Ru_4(CO)_{11}\{\mu-P(CF_3)_2\}_4]$ (3). Reaction with $[(\mu-H)_4Ru_4(CO)_{12}]$ under similar conditions yielded $[(\mu-H)_3Ru_4(CO)_{12}\{\mu-P(CF_3)_2\}]$ (4). All four compounds have been characterised by X-ray crystallography. The fluxional behaviour of the hydrides in 4 has also been studied by variable-temperature NMR spectroscopy. Compounds 1, 2 and 4 were also obtained from the reactions of $[Ru_3(CO)_{12}]$ with $(CF_3)_2PH$ in dichloromethane at 80°C.

Keywords: Ruthenium; Tetra-ruthenium cluster; Tetrakis(trifluoromethyl)disphosphine; Bis(trifluoromethyl)phosphine

1. Introduction

Since the first transition metal complex with a diphosphine ligand was reported by Burg and Mahler in 1958 [1], the chemistry of diphosphines of the form R_2P-PR_2 with monomeric transition metal carbonyls had been extensively developed, especially during the 1960s [2–14]. Generally, dinuclear products were obtained which were either linked through the two phosphorus atoms of a still-intact diphosphine or bridged by a phosphido group formed as a result of P–P bond cleavage.

However, where metal clusters are concerned, very little work has been reported to date. The earliest work reported involved the reaction of $[Fe_3(CO)_{12}]$ with $(CF_3)_2P-P(CF_3)_2$, where a dinuclear complex $[Fe_2(CO)_6\{\mu-P(CF_3)_2\}_2]$ was obtained [15]. More recently, Carty and coworkers have reported the synthesis of the rhomboidal tetraruthenium cluster $[Ru_4(CO)_{10}(\mu-PPh_2)_4]$, as well as the trinuclear cluster $[(\mu_3-H)Ru_3(CO)_6(\mu-PPh_2)_3\{\mu-PPh(C_6H_4)\}]$, from the reactions of $[Ru_3(CO)_{12}]$ with Ph_2P-PPh_2 [16,17]. By using monochlorophosphines as the source of phosphido groups, Carty and coworkers have managed to obtain a

series of rhomboidal tetraruthenium clusters of general formula $[Ru_4(CO)_{13}(\mu-PR_2)_2]$, where R = Ph, ^iPr, OEt, N^iPr_2 and Cy (Cy = cyclohexyl) [16,18].

As part of our continuing interest with ligands containing trifluoromethyl substituents, we have studied the reactions of the diphosphine $(CF_3)_2P-P(CF_3)_2$, as well as the phosphine $(CP_3)_2PH$, with the ruthenium clusters $[Ru_3(CO)_{12}]$ and $[(\mu-H)_4Ru_4(CO)_{12}]$.

2. Results and discussion

The ligand $(CF_3)_2P-P(CF_3)_2$ is stable up to 280°C when pyrolysed [19]. In the presence of metal clusters, however, P–P bond cleavage was observed at 140°C to give a series of tetraruthenium clusters containing one or more bridging phosphido groups. $(CF_3)_2PH$ was also found to undergo P–H cleavage to give the same series of tetraruthenium clusters when reacted with $[Ru_3(CO)_{12}]$ at 80°C.

2.1. Reaction of $(CF_3)_2P-P(CF_3)_2$ with ruthenium clusters

The diphosphine $(CF_3)_2P-P(CF_3)_2$ had been found to react with an equimolar quantity of $[Ru_3(CO)_{12}]$ in p-xylene at 140°C to afford the following major prod-

---

* Corresponding author.

Table 1

Infrared data (cm^{-1}) in hexane (unless otherwise stated) for the (CF$_3$)$_2$P-substituted tetraruthenium carbonyl clusters

Complex	ν(CO)	ν(CF$_3$)
[Ru$_4$(CO)$_{13}${μ-P(CF$_3$)$_2$}$_2$] (1)	2103 (s), 2072 (vs), 2060 (s), 2051 (s), 2036 (vs), 2018 (m)	1179 (w), 1150 (vw), 1132 (w)
[Ru$_4$(CO)$_{14}${μ-P(CF$_3$)$_2$}$_2$] (2)	2112 (w), 2057 (s), 2001 (w)	1173 (vw), 1146 (vw), 1130 (w,sh)
[Ru$_4$(CO)$_{11}${μ-P(CF$_3$)$_2$}$_4$] ^{a} (3)	2113 (m), 2072 (vs), 2044 (w), 1988 (w)	1198 (w), 1179 (w), 1148 (w), 1130 (w)
[(μ-H)$_3$Ru$_4$(CO)$_{12}${μ-P(CF$_3$)$_2$}] (4)	2014 (vw), 2088 (vs), 2075 (vs), 2039 (s), 2033 (m), 2020 (vw), 2011 (w)	1176 (w), 1147 (w), 1132 (w)

^{a} Spectrum taken in CHCl$_3$.

ucts: a red compound [Ru$_4$(CO)$_{13}${μ-P(CF$_3$)$_2$}$_2$] (1), an orange compound [Ru$_4$(CO)$_{14}${μ-P(CF$_3$)$_2$}$_2$] (2) and another red compound [Ru$_4$(CO)$_{11}${μ-P(CF$_3$)$_2$}$_4$] (3). The spectroscopic data of these compounds are given in Tables 1 and 2. The result of this reaction is very different from that of Ph$_2$P–PPh$_2$ with [Ru$_3$(CO)$_{12}$] in p-xylene at 120°C done by Carty and coworkers [16], where only one major product was obtained: a red electron-rich tetraruthenium cluster, [Ru$_4$(CO)$_{10}$(μ-PPh$_2$)$_4$], which has a flat rhomboidal structure. Further structural differences of this compound compared with 3 are highlighted below in Section 2.4. Compound 1, however, is similar to [Ru$_4$(CO)$_{13}$(μ-PR$_2$)$_2$] (R = Ph, ^{i}Pr, OEt, N^{i}Pr$_2$); the whole series of compounds were obtained by Carty and coworkers through reaction of K$_2$[Ru$_4$(CO)$_{13}$] with the appropriate R$_2$PCl [18]. Compound 2 is structurally similar to [Ru$_4$(CO)$_{14}${μ-As(CF$_3$)$_2$}$_2$] which had been obtained in the reaction of (CF$_3$)$_2$AsN$_3$ with [Ru$_3$(CO)$_{12}$] in p-xylene at 135°C [20]. X-Ray crystallographic studies were carried out on crystals grown from ethyl acetate/hexane mixtures for 1 and 3 and from a dichloromethane/hexane mixture for 2.

The reaction of the diphosphine with [(μ-H)$_4$Ru$_4$(CO)$_{12}$] was carried out under the same condi-

tions as above to afford two major compounds, one of which was identified as 1 from its IR and NMR (^{1}H, ^{19}F, ^{31}P) data while the other was identified by NMR spectroscopy (^{1}H, ^{19}F, ^{31}P) and single-crystal X-ray analysis as [(μ-H)$_3$Ru$_4$(CO)$_{12}${μ-P(CF$_3$)$_2$}] (4). The spectroscopic data of 4 are given in Tables 1 and 2. The arsenic analogue, [(μ-H)$_3$Ru$_4$(CO)$_{12}${μ-As(CF$_3$)$_2$}], had been obtained from the reaction of (CF$_3$)$_2$AsGeH$_3$ with [Ru$_3$(CO)$_{12}$] in refluxing p-xylene for 8 h [21].

2.2. Reactions of (CF$_3$)$_2$PH with [Ru$_3$(CO)$_{12}$]

Two different reactions were carried out both in dichloromethane and at 80°C. In one reaction, the cluster-to-ligand ratio used was 1 : 1 and the products obtained were characterised by IR and NMR (^{1}H, ^{19}F, ^{31}P) data to be 1 and 4. In the second reaction, the cluster-to-ligand ratio used was 1 : 2 and compounds 1 and 2 were obtained, as shown by IR and NMR (^{1}H, ^{19}F, ^{31}P) data.

2.3. Infrared spectra of compounds 1, 2, 3 and 4

The absorptions of the carbonyl stretchings generally fall in the region between 2200–1900 cm^{-1}, indicating

Table 2

NMR data (ppm) in CDCl$_3$ (unless otherwise stated) for the (CF$_3$)$_2$P-substituted tetraruthenium carbonyl clusters

Complex	^{1}H	^{31}P-{^{1}H}	^{19}F
[Ru$_4$(CO)$_{13}${μ-P(CF$_3$)$_2$}$_2$] ^{a} (1)	–	144.62 (m)	23.83 (m)
[Ru$_4$(CO)$_{14}${μ-P(CF$_3$)$_2$}$_2$] (2)	–	51.77 (m)	19.46 (d) (J_{P-F} = 59 Hz)
[Ru$_4$(CO)$_{11}${μ-P(CF$_3$)$_2$}$_4$] (3)	–	132.87 (m); 41.18 (m)	23.11 (m); 26.47 (d) (J_{P-F} = 78 Hz)
[(μ-H)$_3$Ru$_4$(CO)$_{12}${μ-P(CF$_3$)$_2$}] (4)	−18.44 (d) (J_{P-H} = 12 Hz)	68.17 (q of sept) ^{b} (J_{P-F} = 53 Hz) (J_{P-H} = 11 Hz)	18.90 (d) (J_{P-F} = 51 Hz)

^{a} Spectrum taken in acetone-d^6. ^{b} Proton-coupled ^{31}P spectrum.

that all the carbonyls are terminal. It has also been observed that for clusters with ligands containing trifluoromethyl substituents, the carbonyl stretchings occur at higher frequency. This is probably due to the greater π-acidity of the ligand as a result of the electron-withdrawing effect of the trifluoromethyl groups. The C–F stretching frequencies due to the trifluoromethyl groups present are also observed at $1100–1200$ cm^{-1} (see Table 1). The C–F deformation frequency at 748 cm^{-1} was not observed due to its weak intensity.

2.4. Crystal structure determination of 1, 2, 3 and 4

The molecular structures of $[Ru_4(CO)_{13}\{\mu\text{-}P(CF_3)_2\}_2]$ (1), $[Ru_4(CO)_{14}\{\mu\text{-}P(CF_3)_2\}_2]$ (2), $[Ru_4(CO)_{11}\{\mu\text{-}P(CF_3)_2\}_4]$ (3) and $[(\mu\text{-}H)_3Ru_4(CO)_{12}\{\mu\text{-}P(CF_3)_2\}]$ (4) are shown in Figs. 1, 2, 3 and 4, respectively, while their atomic coordinates and selected bond lengths and angles are given in Tables 3–10.

The Ru_4P_2 framework in 1 lies on a mirror plane and can be described as having a distorted rhomboid-like structure containing two bridging phosphido groups (see Fig. 1). The cluster is electron-rich with a formal electron count of 64 electrons and five M–M bonds [18]. This is structurally similar to the series of flat rhomboidal tetraruthenium clusters obtained by Carty and coworkers [18], except that here we have one unusually long Ru–Ru bond [i.e. Ru1–Ru4 = 3.374(3) Å]. The Ru–Ru bond, across which the other phosphido group is bridging, is also elongated [Ru3–Ru4 = 3.147(3) Å]. Of the three Ru–Ru bonds forming the triangle which contains no bridging ligands (i.e. Ru1–Ru2–Ru3), Ru1–Ru3 is the longest [3.077(3) Å]; this is consistent with the observation that the substitution of a CO group
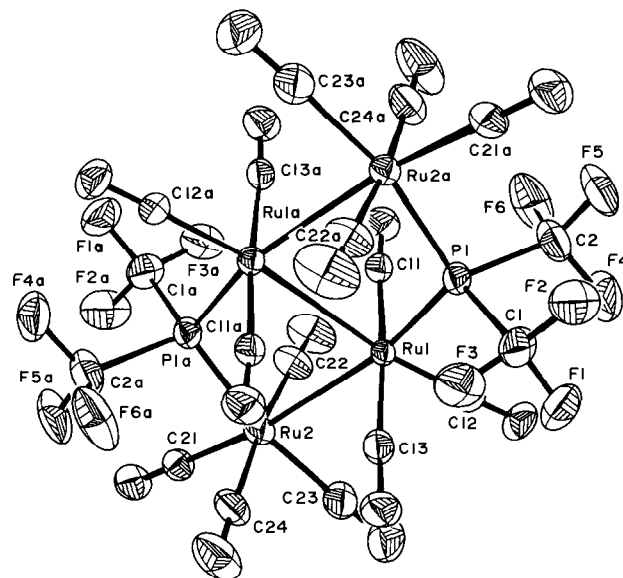

Fig. 2. The molecular structure of $[Ru_4(CO)_{14}\{\mu\text{-}P(CF_3)_2\}_2]$ (2) showing the atom labelling scheme.

by a σ-donating ligand at the equatorial position usually results in the lengthening of the Ru–Ru bond cis to it [22]. The other two Ru–Ru bonds at 2.869(3) Å and 2.913(3) Å, are within the 'normal' range for an Ru–Ru bond length (considered to be between 2.70–2.95 Å) [18]. The Ru2 atom has an approximately octahedral geometry while the other Ru atoms are seven-coordinate and have approximately pentagonal bipyramid geometry. Both phosphorus atoms are bridging asymmetrically with Ru–P–Ru angles of 94.5(2)° and 85.7(1)° for Ru1–P1–Ru4 and Ru3–P2–Ru4, respectively. The average Ru–P distance is 2.305(5) Å and this is compara-

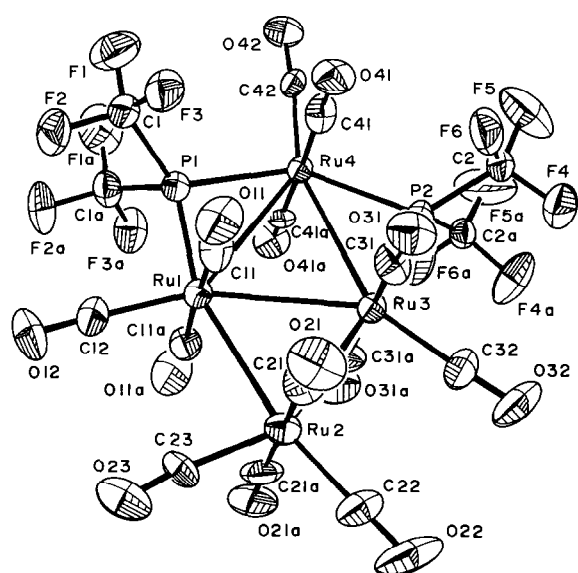

Fig. 1. The molecular structure of $[Ru_4(CO)_{13}\{\mu\text{-}P(CF_3)_2\}_2]$ (1) showing the atom labelling scheme.
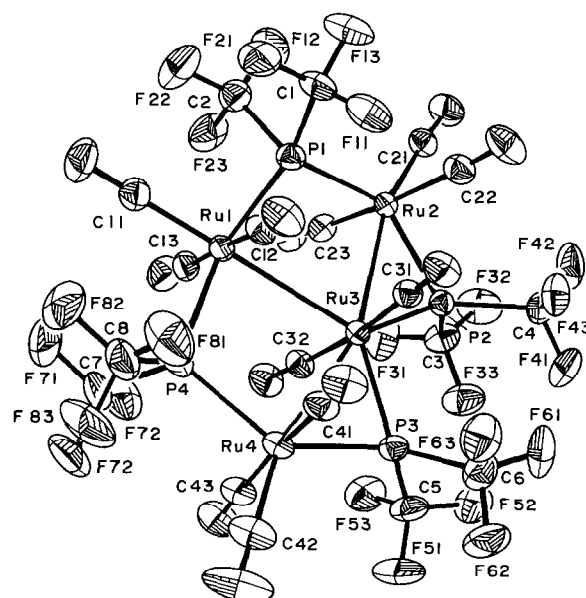

Fig. 3. The molecular structure of $[Ru_4(CO)_{11}\{\mu\text{-}P(CF_3)_2\}_4]$ (3) showing the atom labelling scheme.

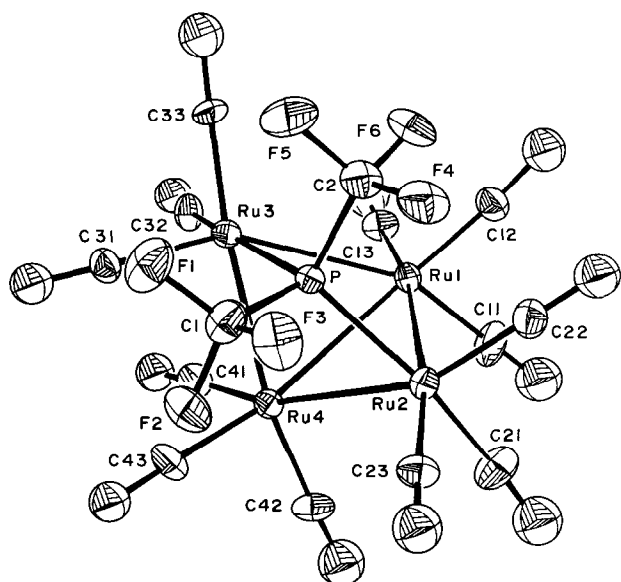Fig. 4. The molecular structure of [(μ-H)₃Ru₄(CO)₁₂{ μ-P(CF₃)₂}] (4) showing the atom labelling scheme.

2.339, 2.354 and 2.372 Å, respectively) [18]. This shortening is due to the electron-withdrawing effects of the trifluoromethyl groups leading to increased π-acidity of the phosphorus atom and hence a shorter Ru–P bond length. Whereas the Ru₄P₂ framework here lies on a mirror plane, in the compounds obtained by Carty and coworkers the phosphorus atoms show a slight but significant deviation from the plane formed by the Ru atoms [18].

The Ru atoms of 2 are planar and are linked in an open chain in a zigzag manner with two phosphido groups bridging across the 1,3- and 2,4-positions of the Ru chain. The phosphorus atoms show a significant deviation from the Ru2aRu1Ru1aRu2 plane (dihedral angle 12.3°) such that the phosphorus and ruthenium atoms taken together show a chair-like conformation. The arsenic analogue, [Ru₄(CO)₁₄{ μ-As(CF₃)₂}₂] [20], has the same planar arrangement of Ru atoms with the arsenic atoms showing a similar deviation from the plane of Ru atoms (dihedral angle 12.5°). While the Ru–Ru bond lengths are within the 'normal' range for compound 2, the bond between the middle two Ru atoms (i.e. Ru1–Ru1a) showed a slight elongation [2.985(2) Å] in the arsenic analogue. In this case, all the Ru atoms have approximately octahedral geometry. The

ble to that in [Ru₄(CO)₁₃{ μ-P(OEt₂)}₂] [average Ru–P = 2.294(8) Å] but shorter than those in [Ru₄(CO)₁₃(μ-PR₂)₂] where R = Ph, ᴵPr and NᴵPr₂ (average Ru–P =

Table 3
Atomic coordinates for [Ru₄(CO)₁₃{ μ-P(CF₃)₂}₂] (1)

Atom	x	y	z
Ru1	0.25	0.09534(7)	0.40
Ru2	0.25	0.11152(9)	0.6135(1)
Ru3	0.25	0.24444(7)	0.4988(2)
Ru4	0.25	0.24757(7)	0.2634(2)
P1	0.25	0.1253(2)	0.2344(4)
P2	0.25	0.3369(2)	0.3854(4)
F1	0.137(1)	0.1062(8)	0.062(1)
F2	0.1338(9)	0.0162(5)	0.156(1)
F3	0.0370(8)	0.1076(6)	0.191(1)
F4	0.124(1)	0.4317(8)	0.4841(9)
F5	0.136(1)	0.4557(8)	0.330(1)
F6	0.0359(8)	0.3730(5)	0.380(1)
C1	0.134(1)	0.0867(7)	0.156(1)
C2	0.136(1)	0.4032(6)	0.394(1)
C11	0.092(1)	0.0953(7)	0.405(2)
C12	0.25	−0.006(1)	0.385(2)
C21	0.086(2)	0.110(1)	0.615(2)
C22	0.25	0.141(2)	0.751(2)
C23	0.25	0.008(1)	0.620(2)
C31	0.089(1)	0.2391(8)	0.503(2)
C32	0.25	0.296(1)	0.620(2)
C41	0.087(1)	0.2480(6)	0.264(2)
C42	0.25	0.2850(9)	0.131(1)
O11	−0.0042(8)	0.0885(7)	0.408(2)
O12	0.25	−0.0663(7)	0.381(2)
O21	−0.005(1)	0.1063(8)	0.626(2)
O22	0.25	0.162(2)	0.832(2)
O23	0.25	−0.050(1)	0.632(2)
O31	−0.07(1)	0.2411(7)	0.505(2)
O32	0.25	0.328(2)	0.692(1)
O41	−0.005(1)	0.2494(7)	0.259(2)
O42	0.25	0.3029(9)	0.048(1)

Table 4
Selected bond lengths (Å) and bond angles (°) for $[Ru_4(CO)_{13}\{\mu\text{-}P(CF_3)_2\}_2]$ (1)

Ru1–Ru2	2.869(3)	Ru2–Ru3	2.913(3)	Ru4–P1	2.311(5)
Ru1–Ru3	3.077(3)	Ru3–Ru4	3.147(3)	Ru3–P2	2.295(5)
Ru1–Ru4	3.374(3)	Ru1–P1	2.282(5)	Ru4–P2	2.331(5)
Ru1–Ru2–Ru3	64.3(1)	P1–Ru4–P2	145.2(2)		
Ru1–Ru3–Ru2	57.2(1)	Ru1–P1–Ru4	94.5(2)		
Ru2–Ru1–Ru3	58.5(1)	Ru3–P2–Ru4	85.7(1)		

Table 5
Atomic coordinates for $[Ru_4(CO)_{14}\{\mu\text{-}P(CF_3)_2\}_2]$ (2)

Atom	x	y	z
Ru1	0.55289(3)	0.07471(3)	0.46118(3)
Ru2	0.64749(3)	−0.07349(3)	0.36773(3)
Ru3	0.90987(3)	−0.01582(3)	1.03102(3)
Ru4	0.84000(3)	0.08909(3)	0.87230(3)
P1	0.46935(9)	0.15433(9)	0.5625(1)
P2	0.99850(8)	0.10432(9)	0.87149(8)
C1	0.5440(5)	0.2123(5)	0.6556(5)
C2	0.4252(6)	0.2689(5)	0.5134(6)
C3	1.0277(4)	0.23225(4)	0.8802(4)
C4	1.0323(4)	0.0900(4)	0.7502(4)
C11	0.4538(4)	0.0742(4)	0.3711(4)
C12	0.6076(4)	0.1788(4)	0.4054(4)
C13	0.6550(4)	0.0656(4)	0.5463(4)
C21	0.6924(4)	−0.1792(4)	0.2995(4)
C22	0.5709(4)	−0.0329(5)	0.2642(4)
C23	0.7327(5)	0.0234(5)	0.3362(5)
C24	0.7266(4)	−0.1028(5)	0.4745(5)
C31	0.9442(4)	0.0968(4)	1.0968(4)
C32	0.8736(4)	−0.1225(4)	0.9563(4)
C33	0.7994(4)	−0.0235(5)	1.0875(4)
C41	0.8454(4)	−0.0193(4)	0.7906(4)
C42	0.7183(4)	0.0512(4)	0.8985(4)
C43	0.8302(4)	0.1882(4)	0.9608(4)
C44	0.8105(3)	0.1756(4)	0.7728(4)
O11	0.3974(3)	0.0798(3)	0.3170(3)
O12	0.6389(3)	0.2420(3)	0.3751(3)
O13	0.7172(3)	0.0660(3)	0.5943(3)
O21	0.7161(3)	−0.2389(3)	0.2585(3)
O22	0.5353(4)	−0.0093(4)	0.2004(3)
O23	0.7815(4)	0.0797(4)	0.3205(5)
O24	0.7744(4)	−0.1203(4)	0.5315(4)
O31	0.9593(4)	0.1614(4)	1.1389(3)
O32	0.8477(3)	−0.1868(3)	0.9191(3)
O33	0.7360(3)	−0.0302(5)	1.1244(4)
O41	0.8426(4)	−0.0783(3)	0.7411(3)
O42	0.6497(3)	0.0288(4)	0.9137(4)
O43	0.8174(3)	0.2473(4)	1.0080(3)
O44	0.7923(3)	0.2278(3)	0.7185(3)
F1	0.6093(3)	0.2616(3)	0.6258(3)
F2	0.4973(3)	0.2675(3)	0.7080(3)
F3	0.5817(3)	0.1456(3)	0.7084(3)
F4	0.4907(4)	0.3275(3)	0.4938(4)
F5	0.3721(3)	0.3147(3)	0.5654(4)
F6	0.3775(4)	0.2521(3)	0.4381(3)
F7	1.0078(3)	0.2652(2)	0.9604(2)
F8	0.9818(3)	0.2855(2)	0.8196(2)
F9	1.1145(3)	0.2489(3)	0.8718(3)
F10	1.0263(3)	0.0004(3)	0.7273(2)
F11	1.1153(3)	0.1165(4)	0.7387(2)
F12	0.9796(3)	0.1380(3)	0.6906(2)

phosphido groups bridge across non-bonded Ru atoms [Ru $\cdots$ Ru = 4.045(1) Å] asymmetrically. The large Ru–P–Ru bond angle of 118.9(1)° is consistent with the absence of an M–M bond [23]. In the case of the arsenic analogue, the non-bonded Ru–Ru distance is 4.229 Å while the Ru–As–Ru bond angle is 124.4(1)°. The average Ru–P bond length in this case is 2.348(2) Å.

In 3 the four Ru atoms almost lie in a plane. Although it has an electron count of 66 and three M–M bonds, 3 does not have the same structure as 2; the Ru atoms are arranged in a 'fan' shape and this is a new structural type for tetrameric clusters having 66 electrons and three M–M bonds. All Ru–Ru bond lengths are elongated with the bond not bridged by any ligand [i.e. Ru1–Ru3: 3.119(2) Å] being about 0.16 Å longer than the rest. This is in exact contrast to the rhomboidal structure of [Ru$_4$(CO)$_{10}$(μ-PPh$_2$)$_4$] reported by Carty and coworkers [16], where the Ru–Ru bond is shortest where there is no bridging ligand (ca. 0.2 Å shorter than the rest). All the Ru atoms have approximately octahedral geometry except for Ru3 which again, like Ru3 in 1, is seven-coordinate. The two phosphido groups spanning the non-bonded Ru atoms form asymmetrical bridges, whereas the other two bridge symmetrically across the bonded Ru atoms. The average distance between the non-bonded Ru atoms is 3.871 Å while the average Ru–Ru distance (containing bridging phosphido groups) is 2.958(2) Å. The average Ru–P–Ru bond angles are 109.6(1)° and 80.6(1)° for the phosphido groups spanning non-bonded and bonded Ru atoms, respectively. The average Ru–P bond lengths for phosphido groups spanning non-bonded Ru atoms is 2.375(2) Å. However, the average Ru–P bond length for phosphido groups across bonded Ru atoms is only 2.287(2) Å; this is shorter than that reported for [Ru$_4$(CO)$_{10}$(μ-PPh$_2$)$_4$] [average Ru–P = 2.337(2) Å]. The phosphorus atoms are not coplanar with the Ru atoms (dihedral angle between 5.4–17.0°), whereas in [Ru$_4$(CO)$_{10}$(μ-PPh$_2$)$_4$] the Ru$_4$P$_4$ core is rigorously planar [16].

The cluster 4 has a butterfly structure with the phosphido group bridging across the wing tips [Ru $\cdots$ Ru = 3.828(1) Å]. This structure is consistent with its electron count of 62 and the presence of five M–M bonds. Two of the hinge-to-wing tip Ru–Ru bonds are nearly normal [average 2.873(1) Å] while the other two are elon-

gated [average 3.050(1) Å]. The hinge Ru atoms also have a slightly longer bond length of 2.946(1) Å. These elongated bond distances are attributed to the presence of bridging hydrides across the affected Ru atoms (i.e. between Ru1–Ru3, Ru1–Ru4 and Ru2–Ru4). Further evidence for the location of the hydrides is provided by the variable-temperature ^{1}H NMR study of this compound (see Section 2.5). There is no direct metal–metal bond across the wing tip Ru atoms and, as a result, the Ru–P–Ru angle is large at 110.9(1)°. The average Ru–P bond length is 2.324(2) Å. The arsenic analogue, [(μ-H)$_3$Ru$_4$(CO)$_{12}$(μ-As(CF$_3$)$_2$)], is structurally similar. In this case, compound 4 has a longer non-bonded Ru–Ru distance as compared to the arsenic analogue. The reverse situation has been seen in the case of compound 2; hence, the Ru–Ru bond distance does not depend only on the size of the Group 15 atom present.

In all four compounds, the Ru–C–O bond angles range from 172–179°, indicating that all carbonyls are terminal, thus supporting the evidence given by the infrared spectra.

2.5. NMR spectroscopic studies of compounds 1, 2, 3 and 4

^{31}P NMR — The ^{31}P NMR data for these compounds generally show high-field chemical shifts for phosphido groups bridging non-bonded Ru atoms (ca. δ 51.77 ppm for 2, 41.18 ppm for 3 and 68.17 ppm for 4) while a shift to lower field was observed when Ru–Ru bonds were present (ca. δ 144.62 ppm for 1 and 132.87 ppm for 3). This is consistent with observations for other metal complexes containing bridging phosphido groups [23].

^{19}F NMR — In compound 1, a large P–Ru–P angle of 145.2(2)° suggests the possibility of strong P–P coupling. such P–P coupling is a maximum when the P–M–P angle is 180° and decreases as the P–M–P angle decreases, until it is zero when the P–M–P angle is 90°; when the P–M–P angle is 180°, there is complete virtual coupling giving rise to a virtual triplet [24]. Due to the effect of incomplete virtual coupling, the ^{19}F NMR spectrum of 1 showed a multiplet. A similar effect was observed with compound 3; the large P–Ru–P bond angle of 165.2(1)° for the pair of phosphorus atoms bridging non-bonded Ru atoms suggested that

Table 6
Selected bond lengths (Å) and bond angles (°) for [Ru$_4$(CO)$_{14}$(μ-P(CF$_3$)$_2$)$_2$] (2)

Ru1–Ru1A	2.935(1)	Ru2–P1A	2.384(2)
Ru1–Ru2	2.941(1)	Ru1–P1	2.312(2)
Ru1 $\cdots$ Ru2A	4.045(1)	Ru2A–P1	2.384(2)
Ru1A $\cdots$ Ru2	4.045(1)		
Ru1A–Ru1–Ru2	87.0(1)	Ru2–Ru1–P1	162.9(1)
Ru1–P1–Ru2A	118.9(1)	Ru1A–Ru1–P1	77.1(1)

Table 7
Atomic coordinates for $[Ru_4(CO)_{11}\{\mu\text{-}P(CF_3)_2\}_4]$ (3)

Atom	x	y	z
Ru1	0.28258(7)	0.36377(5)	0.06921(2)
Ru2	0.24863(6)	0.06925(4)	0.08452(2)
Ru3	0.23010(6)	0.23338(4)	0.14647(2)
Ru4	0.23135(7)	0.44398(5)	0.18080(2)
P1	0.3285(2)	0.1991(2)	0.04197(6)
P2	0.1840(2)	0.0611(2)	0.14971(6)
P3	0.2189(2)	0.2878(2)	0.21264(6)
P4	0.2317(2)	0.5032(2)	0.11289(7)
C11	0.3112(9)	0.4431(6)	0.0222(3)
C12	0.4935(9)	0.3792(6)	0.0915(2)
C13	0.071(1)	0.3477(6)	0.0485(3)
C21	0.2282(8)	−0.0623(6)	0.0576(2)
C22	0.453(1)	0.0263(6)	0.1046(3)
C23	0.0429(8)	0.0953(6)	0.0610(2)
C31	0.4451(8)	0.2203(6)	0.1564(2)
C32	0.0240(9)	0.2612(6)	0.1297(2)
C41	0.450(1)	0.4394(6)	0.1881(2)
C42	0.249(1)	0.5609(7)	0.2172(4)
C43	0.016(1)	0.4597(6)	0.1781(3)
C1A	0.531(1)	0.1866(6)	0.0341(3)
C1B	0.251(1)	0.1864(7)	−0.0146(3)
C2A	−0.006(1)	0.0087(7)	0.1557(3)
C2B	0.294(1)	−0.0259(6)	0.1888(3)
C3A	0.051(1)	0.2556(8)	0.2393(3)
C3B	0.366(1)	0.2516(8)	0.2569(3)
C4A	0.053(1)	0.5738(8)	0.0910(4)
C4B	0.360(1)	0.6172(7)	0.1098(4)
O11	0.3248(8)	0.4886(6)	−0.0066(2)
O12	0.6150(7)	0.3923(5)	0.1019(2)
O13	−0.0481(7)	0.3412(5)	0.0347(2)
O21	0.2166(7)	−0.1415(5)	0.0440(2)
O22	0.5669(7)	−0.0071(6)	0.1148(2)
O23	−0.0731(6)	0.1039(5)	0.0450(2)
O31	0.5707(6)	0.2099(4)	0.1628(2)
O32	−0.1001(6)	0.2774(5)	0.1189(2)
O41	0.5748(6)	0.4415(5)	0.1934(2)
O42	0.2626(8)	0.6268(7)	0.2389(3)
O43	0.1067(7)	0.4749(5)	0.1786(2)
F1A	0.6178(5)	0.1855(4)	0.0702(2)
F1B	0.2761(8)	0.0979(5)	−0.0307(2)
F2A	0.5771(6)	0.2642(4)	0.0121(2)
F2B	0.2965(8)	0.2589(5)	−0.0383(2)
F3A	0.5563(6)	0.0986(4)	0.0147(2)
F3B	0.1032(7)	0.1986(5)	−0.0185(2)
F4A	0.1093(6)	0.0550(5)	0.1293(2)
F4B	0.2427(7)	−0.0295(4)	0.2247(2)
F5A	−0.0152(7)	−0.0903(4)	0.1483(2)
F5B	0.2978(7)	−0.1212(4)	0.1752(2)
F6A	−0.0448(7)	0.0221(5)	0.1928(2)
F6B	0.4353(6)	0.0063(4)	0.1959(2)
F7A	0.0323(7)	0.3230(5)	0.2679(2)
F7B	0.3751(8)	0.1531(4)	0.2649(2)
F8A	0.0637(7)	0.1639(5)	0.2568(2)
F8B	0.3464(7)	0.3016(6)	0.2912(2)
F9A	−0.0696(6)	0.2551(5)	0.2118(2)
F9B	0.4998(7)	0.2804(5)	0.2478(2)
F10A	0.0558(8)	0.6025(6)	0.0527(2)
F10B	0.4992(8)	0.5894(4)	0.1236(2)
F11A	−0.0613(6)	0.5108(5)	0.0915(2)
F11B	0.3648(9)	0.6463(5)	0.0700(2)
F12A	0.0292(8)	0.6557(5)	0.1137(2)
F12B	0.3283(8)	0.6973(4)	0.1292(3)

Table 8
Selected bond lengths (Å) and bond angles (°) for $[Ru_4(CO)_{11}\{\mu\text{-}P(CF_3)_2\}_4]$ (3)

Ru1–Ru3	3.119(2)	Ru1–P1	2.379(2)	Ru2–P2	2.287(2)
Ru2–Ru3	2.961(2)	Ru2–P1	2.361(2)	Ru3–P2	2.281(2)
Ru3–Ru4	2.956(2)	Ru1–P4	2.380(2)	Ru3–P3	2.291(2)
Ru1 · · · Ru2	3.873(2)	Ru4–P4	2.351(3)	Ru4–P3	2.290(2)
Ru1 · · · Ru4	3.869(2)				
Ru1–Ru3–Ru2	79.1(1)	Ru3–P3–Ru4	80.4(1)		
Ru1–Ru3–Ru4	79.1(1)	Ru1–P4–Ru4	109.7(1)		
Ru2–Ru3–Ru4	158.2(1)	P1–Ru1–P4	165.2(1)		
Ru1–P1–Ru2	109.6(1)	P2–Ru3–P3	103.1(1)		
Ru2–P2–Ru3	80.8(1)				

P–P coupling was strong and, as a result, the ^{19}F nuclei on the trifluoromethyl groups of these phosphido ligands showed a multiplet at δ 23.11 ppm. The P–P coupling was weak between the other two phosphorus atoms which form a P–M–P angle of 103.1°; the doublet at δ 26.47 ppm is therefore assigned to the ^{19}F nuclei on the trifluoromethyl group of these phosphorus

atoms. The phosphorus atoms in 2 are three bonds away from each other and no significant coupling occurs between them; as a result, the fluorine atoms show a simple doublet at δ 19.46 ppm ($J_{P-F} = 59$ Hz) in the ^{19}F NMR spectrum. In 4, where there is only one phosphorus atom, a simple doublet was observed at δ 18.90 ppm ($J_{P-F} = 51$ Hz). In these compounds, it was

Table 9
Atomic coordinates of $[(\mu\text{-}H)_3Ru_4(CO)_{12}\{\mu\text{-}P(CF_3)_2\}]$ (4)

Atom	x	y	z
Ru1	0.37453(9)	0.00	0.94822(8)
Ru2	0.5128(1)	−0.10580(8)	0.77525(9)
Ru3	0.15639(9)	0.05389(8)	0.64434(8)
Ru4	0.49499(9)	0.09381(8)	0.74103(9)
P	0.2577(3)	−0.0799(2)	0.6030(3)
C1	0.252(2)	−0.0956(9)	0.407(1)
F1	0.114(1)	−0.0744(7)	0.3080(8)
F2	0.367(1)	−0.0460(6)	0.3842(8)
F3	0.286(1)	−0.1784(5)	0.3789(9)
C2	0.110(2)	−0.1716(8)	0.595(1)
F4	0.166(1)	−0.2508(5)	0.582(1)
F5	−0.0314(8)	−0.1621(6)	0.4823(9)
F6	0.071(1)	−0.1714(6)	0.7160(9)
C11	0.568(2)	−0.011(1)	1.109(1)
C12	0.283(2)	−0.0978(9)	1.004(1)
C13	0.287(1)	0.0864(9)	1.047(1)
C21	0.720(1)	−0.097(1)	0.926(2)
C22	0.456(2)	−0.2087(9)	0.848(1)
C23	0.603(1)	−0.1600(8)	0.645(1)
C31	0.127(2)	0.1054(9)	0.456(1)
C32	0.116(2)	0.1648(8)	0.729(1)
C33	−0.065(1)	0.0170(8)	0.591(1)
C41	0.440(2)	−0.1553(7)	0.754(1)
C42	0.722(1)	0.114(1)	0.842(2)
C43	0.504(2)	0.1161(8)	0.551(1)
O11	0.680(1)	−0.0138(9)	0.211(1)
O12	0.219(1)	−0.1558(8)	1.04000(1)
O13	0.241(1)	0.1369(8)	1.10902(1)
O21	0.851(2)	−0.0936(9)	1.00996(1)
O22	0.418(1)	−0.2744(8)	0.887(1)
O23	0.659(1)	−0.1952(8)	0.57014(1)
O31	0.106(1)	0.1352(8)	0.34625(1)
O32	0.084(1)	0.2252(7)	0.780(1)
O33	−0.195(1)	−0.0041(8)	0.561(1)
O41	0.412(1)	0.2853(7)	0.766(1)
O42	0.855(2)	0.125(1)	0.906(2)
O43	0.517(1)	0.129(7)	0.440(1)

Table 10
Selected bond lengths (Å) and bond angles (°) for [(μ-H)$_3$Ru$_4$(CO)$_{12}$(μ-P(CF$_3$)$_2$)] (4)

Ru1–Ru2	2.881(1)	Ru2–Ru4	3.061(2)	Ru3–P	2.315(3)
Ru1–Ru3	3.039(1)	Ru3–Ru4	2.865(1)	P–C1	1.905(13)
Ru1–Ru4	2.946(1)	Ru2–P	2.332(2)	P–C2	1.887(14)
Ru2···Ru3	3.828(1)				
Ru1–Ru2–Ru4	59.3(1)	Ru1–Ru4–Ru3	63.1(1)	Ru3–P–Ru2	110.9(1)
Ru1–Ru3–Ru4	59.8(1)	Ru2–Ru1–Ru4	63.4(1)		
Ru1–Ru4–Ru2	57.3(1)	Ru3–Ru1–Ru4	57.2(1)		

observed that P–F coupling constants were smaller when Ru–Ru bonds were absent than when Ru–Ru bonds are present [ca. J_{P-F} (without Ru-Ru bond) = 59 Hz for 2 and 51 Hz for 4; J_{P-F} (with Ru–Ru bond) = 78 Hz for 3). A similar observation was made in the case of the triosmium compounds: [{Os$_3$(μ-H)(CO)$_{11}$}{ μ-PH(CF$_3$)}{Os$_3$(CO)$_{11}$}], a cluster consisting of two triosmium framework linked by a phosphido group and [Os$_3$(μ-H)(CO)$_{10}${ μ-PH(CF$_3$)}], a cluster with a phosphido group bridged across bonded Os atoms. The former compound showed a P–F coupling constant of 44 Hz while the latter exhibited a value of 68 Hz [25].

H NMR — The absence of high-field signals in the ^{1}H NMR spectra of compounds 1, 2 and 3 indicated that

metal hydrides were absent. In 4 the coupled ^{31}P NMR spectrum shows the splitting of the septet (obtained in the proton-decoupled spectrum) into a quartet of septets, suggesting the presence of three hydrides in 4. From the structure, it can be seen that two of the hinge-to-wing tip Ru–Ru bond lengths as well as the hinge-to-hinge Ru–Ru bond length are elongated. This implies that the hydrides are probably bridging across these Ru atoms. As the proposed hydride positions imply that two types of hydrides are present, while the room temperature ^{1}H NMR spectrum shows only one doublet in the high-field region (δ − 18.44 ppm, J_{P-H} = 12 Hz), fluxional behaviour of the hydrides is suspected and a variable-temperature NMR study was therefore attempted. The dou-
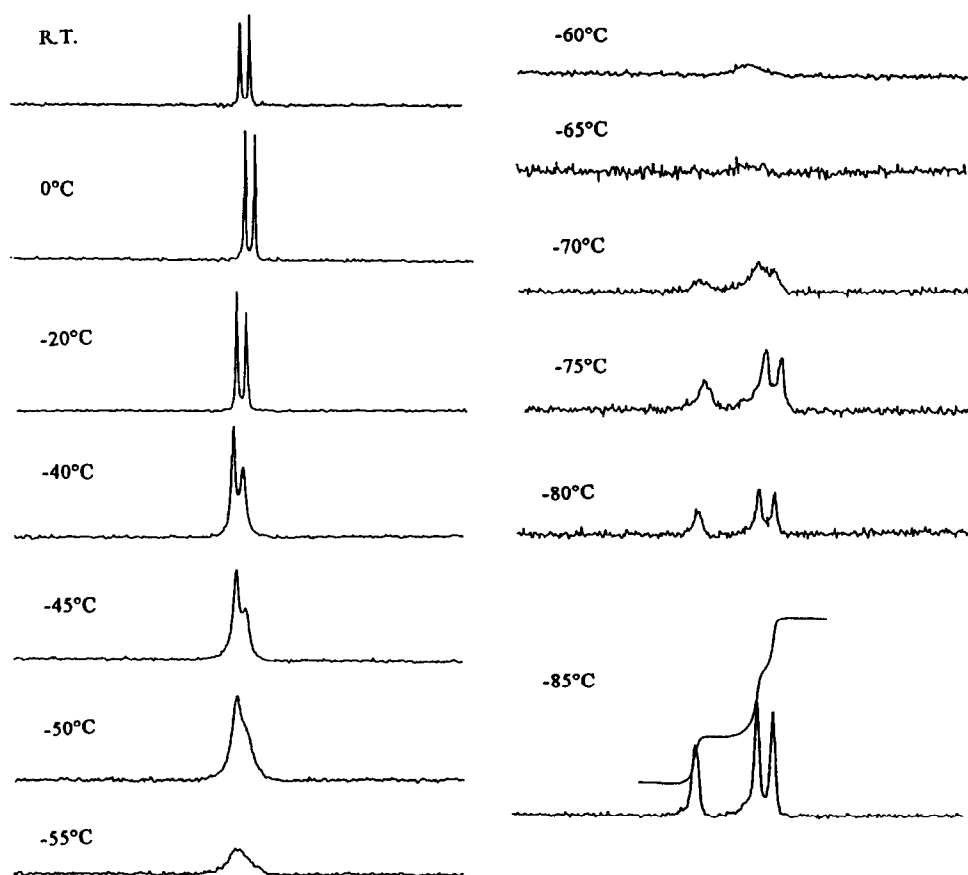

Fig. 5. Variable-temperature ^{1}H NMR spectra of [(μ-H)$_3$Ru$_4$(CO)$_{12}$(μ-P(CF$_3$)$_2$)] (4).

blet was then resolved into a sharp singlet (δ -17.48 ppm) and a doublet (δ -18.45 ppm, $J_{P-H} = 20$ Hz) at $-85°C$ with an integration ratio of $1:2$ (see Fig. 5), which was consistent with the proposed solid-state structure. From the values $\Delta\nu = 86$ Hz and $T_c = -65°C$ (208 K), the free energy of activation for this process was estimated to be 41 kJ mol^{-1} [26]. This is slightly higher than that reported in other tetraruthenium systems where ΔG ranges from 31 to 38 kJ mol^{-1} [26,27].

3. Experimental details

The reactions described above were carried out in evacuated reaction tubes. Dichloromethane was dried over phosphorus pentoxide while p-xylene was dried over sodium wires [28] and both were distilled prior to use. The following compounds were prepared according to literature methods: [Ru$_3$(CO)$_{12}$] [29], [(μ-H)$_4$Ru$_4$(CO)$_{12}$] [30], (CF$_3$)$_2$PH [31] and (CF$_3$)$_2$P–P(CF$_3$)$_2$ [32]. Infrared spectra were recorded on a Perkin-Elmer 983G spectrophotometer; ^{1}H and ^{31}P NMR spectra on a Bruker ACF-300 instrument using SiMe$_4$ (^{1}H) or H$_3$PO$_4$ (^{31}P) as references. ^{19}F NMR spectra were recorded on a JEOL FX-90Q FT instrument using trifluoroacetic acid as reference. The reaction products were separated by thin-layer chromatography (TLC) on 20 cm × 20 cm glass plates coated with 0.3 mm of Merck Kieselgel 60GF silica gel, using either pentane or hexane as eluent.

3.1. Reactions of (CF$_3$)$_2$P–P(CF$_3$)$_2$ with ruthenium clusters

3.1.1. (a) With [Ru$_3$(CO)$_{12}$]

[Ru$_3$(CO)$_{12}$] (218.0 mg, 0.341 mmol) and (CF$_3$)$_2$P–P(CF$_3$)$_2$ (68.2 mg, 0.348 mmol) in p-xylene were heated to 140°C for 18 h, after which a red solution was obtained. on cooling to room temperature, dark red crystals formed in the red solution. The solvent and volatiles were removed under vacuum. The solid products were taken up in dichloromethane to give a red solution together with a red crystalline solid that was only slightly soluble in dichloromethane. This solid was separated from the solution and recrystallised using a mixture of ethyl acetate and hexane to yield red single crystals of compound 3. Yield 8 mg, 2% (Anal. Found: C, 16.36; P, 9.08%. Calc. for C$_{19}$F$_{24}$O$_{11}$P$_4$Ru$_4$: C, 16.44; P, 8.92%). Thin-layer chromatography of the solution using pentane as eluent yielded red-coloured 1 (yield 48 mg, 17%.) (Anal. Found: C, 19.13; P, 5.85%. Calc. for C$_{17}$F$_{12}$O$_{13}$P$_2$Ru$_4$: C, 18.46; P, 5.60%) and orange 2 (yield 19 mg, 6%) (Analysis: Found: C, 19.18; P, 5.69%. Calc. for C$_{18}$F$_{12}$O$_{14}$P$_2$Ru$_4$: C, 19.06; P, 5.46%). Single crystals of 1 were obtained by recrystallisation at low temperature using a ethyl acetate/

hexane mixture as solvent. Those of 2 were obtained from recrystallisation using a dichloromethane/hexane mixture at $-20°C$.

IR (hexane) (cm^{-1}): compound 1: (ν_{CO}) 2103 (s), 2072 (vs), 2060 (s), 2052 (s), 2036 (vs), 2018 (m); (ν_{C-F}) 1179 (w), 1150 (vw), 1132 (w). IR (hexane) (cm^{-1}): compound 2: (ν_{CO}) 2112 (w), 2057 (s), 2001 (w); (ν_{C-F}) 1173 (vw), 1146 (vw), 1130 (w, sh). IR (CHCl$_3$) (cm^{-1}): compound 3: (ν_{CO}) 2113 (m), 2072 (vs), 2044 (w), 1988 (w); (ν_{C-F}) 1198 (w), 1179 (w), 1148 (w), 1130 (w).

NMR (CD$_3$COCD$_3$) δ: ^{31}P-{^{1}H}: (1) 144.62 (m) ppm; ^{19}F: (1) 23.83 (m) ppm. NMR (CDCl$_3$) δ: ^{31}P-{^{1}H}: (2) 51.77 (m) ppm; (3) 132.87 (m); 41.18 (m) ppm; ^{19}F: (2) 19.46 (d, $J_{P-F} = 59$ Hz) ppm; (3) 23.11 (m); 26.47 (d, $J_{P-F} = 78$ Hz) ppm.

3.1.2. (b) With [(μ-H)$_4$Ru$_4$(CO)$_{12}$]

The ligand (CF$_3$)$_2$P–P(CF$_3$)$_2$ (95.1 mg, 0.281 mmol) was condensed at liquid nitrogen temperature into a degassed solution of [(μ-H)$_4$Ru$_4$(CO)$_{12}$] (202.0 mg, 0.273 mmol) in p-xylene. The reaction mixture was heated to 140°C for 3 h to give a dark reddish brown solution. The solvent and volatiles were removed under vacuum. The resultant solid taken up in dichloromethane and chromatographed on silica plates using hexane as eluent yielded two major products: a red compound, identified as 1 (yield 17 mg, 6%) and orange 4 (yield 27 mg, 10%) (Anal. Found: C, 17.75; H, 0.14; P, 4.25%. Calc. for C$_{14}$F$_6$O$_{12}$PRu$_4$: C, 18.43; H, 0.33; P, 3.39%). Crystals of 4 suitable for X-ray crystallography were obtained by recrystallisation from a dichloromethane/hexane mixture at $-20°C$.

IR (hexane) (cm^{-1}): compound 4: (ν_{CO}) 2014 (vw), 2088 (vs), 2075 (vs), 2039 (s), 2033 (m), 2020 (vw), 2011 (w); (ν_{C-F}) 1176 (w), 1147 (w), 1132 (w).

NMR (CDCl$_3$) δ: ^{1}H: (298 K) -18.44 (d) ppm; (188 K) -17.48 (s); 18.45 (d, $J_{P-H} = 20$ Hz) ppm; ^{31}P-{^{1}H}: 68.17 (sept., $J_{P-F} = 53$ Hz) ppm; ^{31}P: 68.17 (q. of sept., $J_{P-F} = 53$ Hz, $J_{P-H} = 11$ Hz) ppm; ^{19}F: 18.90 (d, $J_{P-F} = 51$ Hz) ppm.

3.2. Reaction of (CF$_3$)$_2$PH with [Ru$_3$(CO)$_{12}$]

3.2.1. (a) Ratio of ligand/cluster = 1:1

Into a dichloromethane solution containing [Ru$_3$(CO)$_{12}$] (200.0 mg, 0.313 mmol) was condensed (CF$_3$)$_2$PH (53.7 mg, 0.316 mmol), after which the reaction mixture was heated to 80°C. Complete dissolution of [Ru$_3$(CO)$_{12}$] occurred after 1 h and this was accompanied by a colour change from light orange to red. Heating was continued for another 17 h. Solvent and other volatiles were removed under vacuum. The solid mixture was then dissolved in the minimum of dichloromethane and chromatographed on silica plates, using hexane as eluent, to yield two major products: a

Table 11
Crystallographic data for **1**, **2**, **3** and **4**

Complex	1	2	3	4
Formula	$C_{17}F_{12}O_{13}P_2Ru_4$	$C_{18}F_{12}O_{14}P_2Ru4$	$C_{19}F_{24}O_{11}P_4Ru4$	$C_{14}F_6O_{12}PRu_4$
Formula weight	1106.4	1134.4	1388.3	909.4
Crystal system	orthorhombic	monoclinic	monoclinic	monoclinic
Space group	$Ama2$	$P2_1/c$	$P2_1/c$	$P2_1$
a (Å)	12.075(7)	14.977(2)	9.065(4)	8.788(1)
b (Å)	18.639(9)	14.290(3)	12.988(4)	15.252(2)
c (Å)	13.363(4)	14.858(3)	32.704(13)	9.725(1)
β (°)	90.00(0)	93.37(1)	97.56(4)	109.85(0)
V (Å³)	3003(2)	3174.4(10)	3817(3)	1226.1(3)
Z	4	4	4	2
ρ_{calc} (g cm⁻³)	2.447	2.374	2.416	2.463
μ (cm⁻¹)	22.13	20.99	18.88	25.82
Reflections				
Total	1451	5777	7026	2789
Unique	1451	5546	6593	2636
Observed [a]	1326	4444	4695	2417
No. of variables	241	452	560	274
R (obd. data)	0.0373	0.0303	0.0403	0.0332
R_w (obd. data)	0.0544	0.0367	0.0478	0.0428
Goodness of fit	0.91	1.19	1.05	1.02

[a] $F_0 > 4.0\sigma(F_0)$.

red compound identified as **1** (yield 14 mg, 5%) and an orange compound identified as **4** (yield 42 mg, 20%) whose IR and NMR (^{1}H, ^{19}F, ^{31}P) data were found to be the same as reported above.

3.2.2. (b) Ratio of ligand / cluster = 2 : 1

$(CF_3)_2PH$ (107.0 mg, 0.632 mmol) was condensed at liquid nitrogen temperature into a solution of $[Ru_3(CO)_{12}]$ (200.0 mg, 0.313 mmol) in dichloromethane. The reaction mixture was heated to 80°C. The $[Ru_3(CO)_{12}]$ was completely dissolved after 1 h and the colour of the solution changed from light orange to darker orange. Heating was continued for a further 17 h before solvent and other volatiles were removed under vacuo. The remaining solid was taken up in minimum amount of dichloromethane. Thin-layer chromatography of the reaction products using hexane as eluent yielded two major compounds: red **1** (yield 17 mg, 16%) and orange **2** (yield 22 mg, 8%). The products were found to have the same IR and NMR (^{1}H, ^{19}F, ^{31}P) data as those reported above.

3.3. X-ray structure determination

Crystal data and details of measurement for compounds **1**, **2**, **3** and **4** are given in Table 11. Diffraction intensities were collected at 298 K on a Siemens R3m/V X-ray diffractometer with graphite-monochromatised Mo Kα radiation ($\lambda = 0.71073$ Å), scan range 3.0° < 2θ < 50.0° for **1**, **2** and **3** and 4.0° < 2θ < 53.0° for **4**, and indices $+h$, $+k$, $+l$ for **1**, $+h$, $+k$, $\pm l$ for **2**, $+h$, $+k$, $\pm l$ for **3** and $\pm h$, $+k$, $+l$ for **4**. All computations were carried out using the SHELXTL PLUS (PC

version) program package. The structures were solved by direct methods. Refinement was by the full-matrix, least-squares method with all non-hydrogen atoms being refined anisotropically.

4. Conclusions

In the reactions of the ruthenium clusters $[Ru_3(CO)_{12}]$ and $[(\mu\text{-}H)_4Ru_4(CO)_{12}]$ with $(CP_3)_2P\text{-}P(CF_3)_2$ and $(CF_3)_2PH$, it was observed that P–P or P–H bond cleavage had occurred to give a series of tetraruthenium clusters containing one or more bridging phosphido groups. Furthermore, in compounds **2**, **3** and **4**, the phosphido groups were found to bridge non-bonded Ru atoms while in compound **1** one pair of Ru atoms containing a bridging phosphido group was found to be unusually far apart. The clusters, with the exception of compound **1**, are all electron-precise. These results are different from that obtained by the reaction between equimolar amounts of $Ph_2P\text{-}PPh_2$ and $Ru_3(CO)_{12}$, where only one major product, an electron-rich flat rhomboidal tetraruthenium cluster $[Ru_4(CO)_{10}(\mu\text{-}PPh_2)_4]$, was obtained [16]. This difference in reactivity between the two diphosphines can be attributed to the difference in electronegativity of the substituents on the phosphorus atoms.

Acknowledgements

References and notes

[1] A.B. Burg and W. Mahler, *J. Am. Chem. Soc.*, **80** (1958) 2334.

[2] A.H. Cowley, *Chem. Rev.*, **65** (1965) 617.

[3] A.N. Caminade, J.P. Majoral and R. Mathieu, *Chem. Rev., 91* (1991) 575.

[4] R.G. Hayter, *J. Am. Chem. Soc., 85* (1963) 3120.

[5] W.R. Cullen and R.G. Hayter, *J. Am. Chem. Soc., 86* (1964) 1030.

[6] R.G. Hayter and L.F. Williams, *Inorg. Chem., 3* (1964) 717.

[7] J. Chatt and D.A. Thornton, *J. Chem. Soc.*, (1964) 1005.

[8] J. Chatt and D.A. Thornton, *J. Chem. Soc.*, (1964) 2713.

[9] H.G. Ang and J.M. Miller, *Chem. Ind. (London)*, (1966) 944.

[10] P.S. Braterman and D.T. Thompson, *J. Chem. Soc.*, (1968) 1454.

[11] M. Green, A. Taunton-Rigby and F.G.A. Stone, *J. Chem. Soc.*, (1969) 1875.

[12] G. Beysel, J. Grobe and W. Mohr, *J. Organomet. Chem., 170* (1979) 319.

[13] J. Grobe and D. Le Van, *J. Fluorine Chem., 19* (1982) 279.

[14] A.J.M. Caffyn, M.J. Mays, G.A. Solan, D. Braga, P. Sabatino, G. Conole, M. McPartlin and H.R. Powell, *J. Chem. Soc., Dalton Trans.*, (1991) 3103.

[15] R.C. Dobbie, M.J. Hopkinson and D. Whittaker, *J. Chem. Soc., Dalton Trans.*, (1972) 1030.

[16] G. Hogarth, J.A. Phillips, F. Van Gastel, N.J. Taylor, T.B. Marder and A.J. Carty, *J. Chem. Soc., Chem. Commun.*, (1988) 1570.

[17] J.F. Corrigan, S. Doherty, N.J. Taylor and A.J. Carty, *J. Organomet. Chem., 462* (1993) C24.

[18] (a) J.F. Corrigan, M. Dinardo, S. Doherty, G. Hogarth, J. Sun, N.J. Taylor and A.J. Carty, *Organometallics, 13* (1994) 3572; (b) J.F. Corrigan, M. Dinardo, S. Doherty and A.J. Carty, *J. Cluster Sci., 3* (1992) 313.

[19] W. Mahler and A.B. Burg, *J. Am. Chem. Soc., 80* (1958) 6161.

[20] H.G. Ang and Y.W. Lee, *Proc. 2th ACS Winter Fluorine Conf.*, 22–27 Jan. 1995, St. Petersburg, FL, P46, pp. 58.

[21] H.G. Ang, L.L. Koh and Y.W. Lee, Unpublished results.

[22] M.I. Bruce, M.J. Liddell, C.A. Hughes, B.W. Skelton and A.H. White, *J. Organomet. Chem., 347* (1988) 157.

[23] A.J. Carty, B.A. MacLaughlin and D. Nuciurone, in J.G. Verkade and L.D. Quinn (eds.), *Phosphorus-31 NMR Spectroscopy in Stereochemical Analysis: Organic Compounds and Metal Complexes*, VCH, New York, 1987, Chap. 16.

[24] R.H. Crabtree, *The Organometallic Chemistry of Transition Metals*, 2nd edn., Wiley, London, 1994, Chap. 10, pp. 237–239.

[25] H.G. Ang, C.H. Koh, L.L. Koh, W.L. Kwik, W.K. Leong and W.Y. Leong, *J. Chem. Soc., Dalton Trans.*, (1993) 847.

[26] (a) The equations used for the calculations are (i) $k_c = 2^{1/2}(\pi/2)\Delta\nu$ and (ii) $\Delta G^{\ddagger} = 2.303 RT_c[\log(k_B/h) - \log(k_c/T_c)]/1000$ where $\Delta\nu$ is the chemical shift difference in hertz and T_c is the coalescence temperature; (b) M.R. Churchill, R.A. Lashewycz, J.R. Shapley and S.I. Richter, *Inorg. Chem., 19* (1980) 1277.

[27] A.A. Bahsoun, J.A. Osborn, J.P. Kintzinger, P.H. Bird and U. Siriwardane, *Nouv. J. Chim., 8* (1984) 125.

[28] A.I. Vogel, *Textbook of Practical Organic Chemistry*, 5th edn., Longman, London, UK 1989, Chap. 4, pp. 396–411.

[29] M.I. Bruce, C.M. Jenkins and N.L. Jones, *Inorg. Synth., 26* (1989) 259.

[30] M.I. Bruce and M.L. Williams, *Inorg. Synth., 26* (1989) 262.

[31] R.G. Cavell and R.C. Dobbie, *J. Chem. Soc. A*, (1967) 1308.

[32] F.W. Bennett, H.J. Emeleus and R.N. Haseldine, *J. Chem. Soc. A*, (1953) 1565.